Nonlinear biomechanical analysis of the human upper limb in a outstretched forward fall

Paweł Biesiacki, Jan Awrejcewicz, Jerzy Mrozowski, Krzysztof Woźniak

*Abstract:*In this paper a three dimensional solid finite element model of the human upper limb is subjected to real load during a forward fall. A model of bones with accurate geometry and material properties retrieved form CT scan data is used to carry out the investigation of therealistic mechanical behavior of bone structures. It allows for bones behavior modeling using a computational model in ANSYS and it includes the complete osseous structure while simplifying the cartilage. The load was assumed as triangulared dynamic pulse of a finite duration. The obtained results imply that all models have the same type of global dynamical behavior and strains are located in almost the same places. Apart from the obtained results it has been demonstrated numerically that cancellous bone has a major impact of the strain distribution. Maximum and minimum strains depend on the different Young's modulus defined by the CT scan gray scale. The obtained results will help to analyse properly the common injuries of the upper limb during falls.

1. Introduction

Fall is a common result of the unexpected postural disturbances, such as tripping, slipping, sudden turning, etc., that occurs in all age groups [1-3]. For the more than half of the falls, the direction is forward. In this type of the fall the most common strategy is to use one or both upper limb to regain balance or to arrest fall to avoid risk of the head or thorax injures [2,4].

The upper limb (presented in Figure 1) consists of shoulder region, arm, forearm and hand [5]. The bones of the shoulder girdle are the clavicle and the scapula. The bone of the arm is called the humerus, andits upper end meets the scapula and forms the shoulder joint that permits movements of the arm. Forearm extends from the elbow to the wrist. Upper ends of its bones, radius and ulna, meet the lower end of the humerus to form the elbow joint, while their lower ends meet the carpal bones to forming the wrist joint. The elbow joint permits movements of the forearm, namely flexion and extension. The radioulnarjoint permits two rotatory movements of the forearm called pronation and

supination. Hand originates at wrist, where bones of forearm connect with five metacarpal bones, that form metacarpus or palm. Further located are phalanges that are small bones forming skeleton of fingers and thumb. There are total of 14 phalanges, two for the thumb, and three for each of the fingers. The phalanx that articulates with metacarpal bone is called proximal phalanx, while the terminal one is called distal phalanx. These are the unique phalanges, that thumb contains. In other fingers, here is also middle phalanx located between proximal and distal one. The joints connecting each pair of the phalanges are called interphalangeal joints.

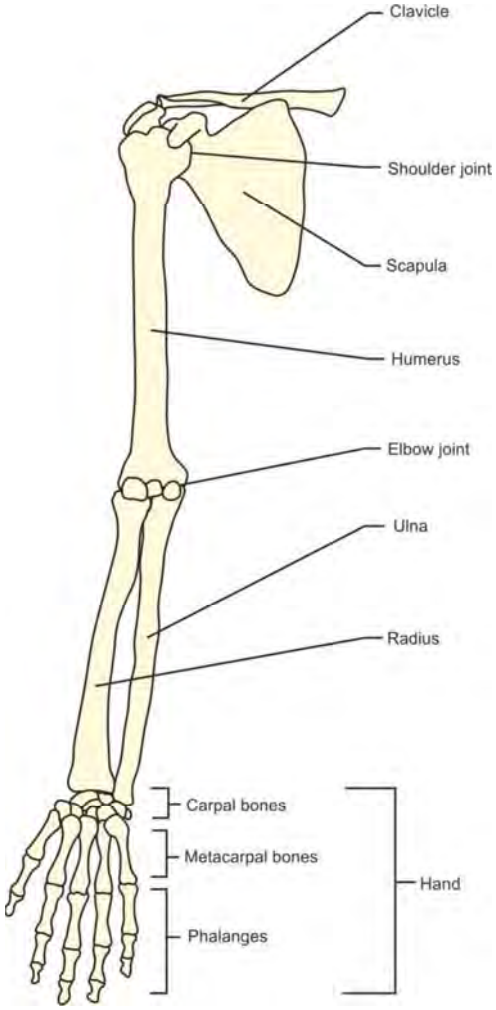

Figure 1. The human upper limb.

In most cases the upper limb is the first body element exposed to dynamical force action generated during the forward fall. This fact implies their particular susceptibility to various kind of injury. The part of the upper limb which run the most risk of getting fracture is the forearm [6].

In this paper we present results of modeling and analysis of the upper limb injury dynamics during fall carried out by the use of finite element method (FEM). Applying MIMICS program to convert the CT scans in DICOM format to the format accepted by FEM packages the realistic three-dimensional model of the upper limb bones was obtained. This model was used for further analysis in ANSYS.

2. Materials and methods

For FEM analysis of the upper limb, firstly the 3D model of bones was developed. Geometrical data of real proximal human upper limb bones is used in the form of Digital Imaging and Communications in Medicine (DICOM) image obtained from CT scan of the a 35 years old man, with a height of 1.73 m and weight 75 kg. As DICOM format contains binary data elements, the CT scan data in the form of DICOM consist of two dimensional gray scaled images. CT images are a pixel map of the linear X-ray attenuation coefficient of tissue. The pixel values are scaled so that the linear X-ray attenuation coefficient of air equals -1024 and that of water equals 0. This scale is called the Hounsfield scale. The Hounsfield Unit (HU), corresponding to each element, is averaged and converted into gray values and then to material properties of bone. Using this scale, fat is around -110, muscle is around 40, trabecular bone is in the range of 80 to 500 and cortical bone ranging from 500 to 900 [7].

The gray-scaled values of the images represent the density of scanned bone. DICOM files are 2D, but they retained data for 3D as well. This DICOM data set obtained from Siemens 64 Slice CT Scanner contains total 274 numbers of slices. The slice thickness is 1.5 mm, pixel size 0,977 mm and resolutions 512 x 512. The CT scan data set is processed using an interpolation algorithm in MIMICS 15 and creates three-dimensional model of upper limb bones by following steps [8]:

a) Thresholding based on Hounsfield Units was done to ensure that segmentation object which contains only those pixels of image with a defined value.
b) The region growing process allows splitting the segmentation in different and separated part.
c) The generated region mask was used to develop 3D model for the bone. The 3D reconstruction is based on 3D interpolation techniques that transform the 2D images in a 3D model. For this reconstruction case, gray values interpolation was used associated with the accuracy algorithm for achieving a more accurate dimensional representation of the upper limb bones.
d) Using MIMICS software, bones were converted into preprocessing files for FEM analysis.

The mechanical properties of the bone vary according to the age, weight, sex and nutritious regimen of each different person. In this study, properties of the bones were calculated using the equations (1) and (2) [9].:

$$\rho = 1{,}067\mathrm{HU} + 131, \tag{1}$$

$$\mathrm{E} = 0{,}004\rho^{2{,}01}, \tag{2}$$

where ρ represents density [kg/m^3], HU is the Hounsfield Units, E denotes Young modulus [MPa] and ν Poisson ratio.

The resulting data obtained for three upper limb bones, i.e. humerus, radius and ulna, are reported in Table 1.

Table 1.Material properties obtained from CT.

	Humerus	Radius	Ulna
E [GPa]	2.7- 15.6	0.6 - 12	1.2 - 12
ν	0.3	0.3	0.3

As shown in Fig. 2, the finite element models were created taking account inhomogeneous material properties based on the CT density.

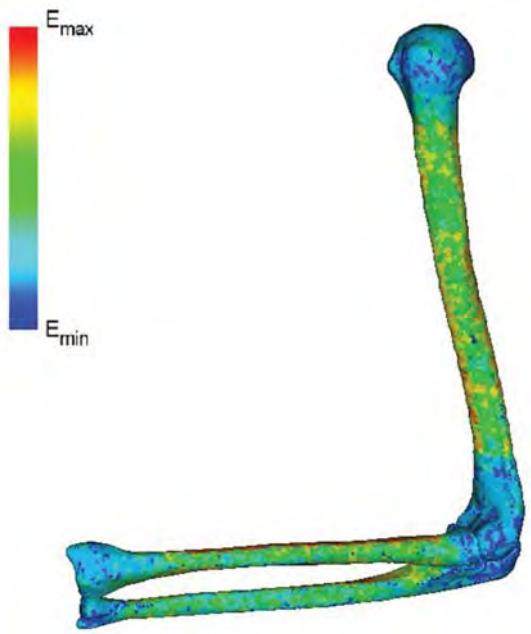

Figure 2. The solid model bones showing inhomogeneous material properties.

As the presented analysis required three-dimensional nonlinear processing, a solid element 185, suitable for this task, was chosen. This tetrahedron element has 8 nodes and three degrees of freedom (UX, UY and UZ) by node. Bones were modeled as an isotropic, linear elastic and inhomogeneous material. The humerus contained 14061 nodes and 79947 elements. The radius contained 5743 nodes and 30829 elements and the ulna contained 6316 nodes and 33973 tetrahedral elements. Using ANSYS three models of upper limb in different forearm positions (Figure 4) were built according to literature data (as shown in Fig. 3).

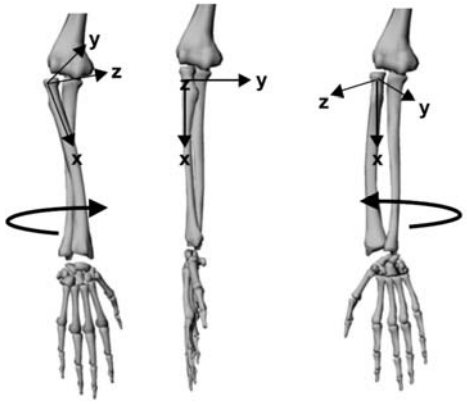

Figure 3. Forearm positions and coordinate system in pronation, neutral state and supination [10].

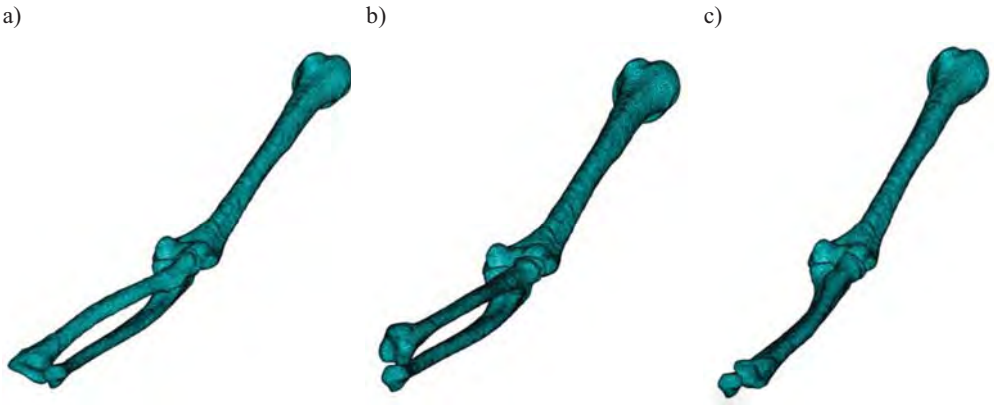

Figure 4. Forearm positions.

By prescribing a rotation angle (as shown in Figure 4) the models of the forearms in pronation, neutral and supination were obtained.

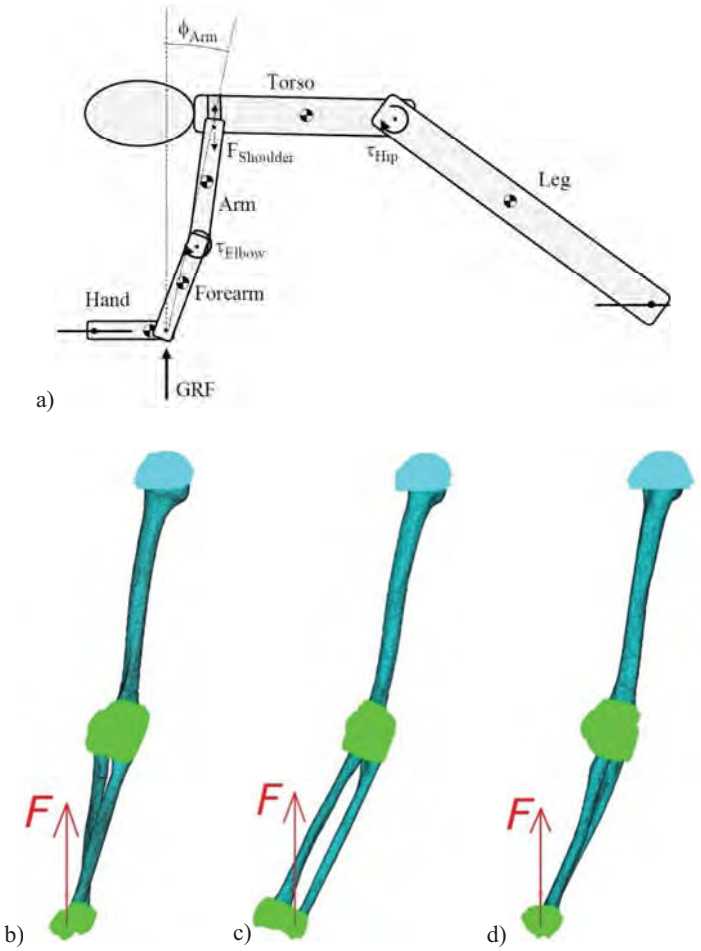

a) Boundary conditions. Model of the symmetric forward fall with arms [11] and positioning of arm bones in layout b) pronation, c) neutral state d) supination.

Boundary conditions were presented in Figure 5. Degree of freedom in proximal humerus were fixed that means UX, UY, UZ=0 (see blue color on photos). The bones in the joints were connected by coupling nodes (see green color). Coupling degrees of freedom into a set causes the results calculated for one member of the set to be the same for all members of the set. A more general form of coupling can be done with constraint equations. For structural analyses, a list of nodes is defined along with the nodal directions in which these nodes are to be coupled. As a result of this coupling, these nodes are forced to take the same displacement in the specified nodal coordinate direction [12], [13]. Curve force – time (Figure 6a, a)) [11] presents the magnitude of the ground reaction force

(GRF) during arrested forward fall to the ground from a 1m shoulder height. Three different arrest strategies: stiff - arm, natural, and minimum impact force was investigated to reduce peak force. To analysis stiff – arm was taken as a the worst case. In this study the GRF was modeled as a tiangulared dynamic force (F) pulse. The angle between the longitudinal axis of the humerus and the force13,5° was taken. Impulse was divided into six load steps. Maximal peak force 1170 N in time 0,01 s was assumed in the first load step. Each of step approximate the real value of ensemble-averaged time the ground reaction force histories. This approach allows in simply way investigate behaviour of upper limb during forward fall.

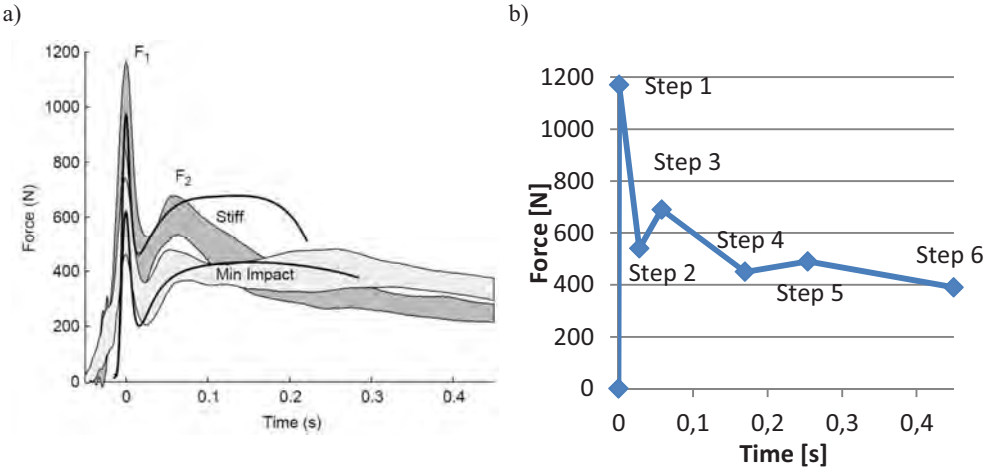

Figure 5. Model of the first phase of the impact for near-straight (174°) elbow angle a) literature model [11] and b) for approximated values.

3. Results

In result of the numerical analysis, there was obtained possibility to present an arbitrary selected values as an function of the strain and stress state in each of the element of the studied system. To predict the locations where fractures can occur it was decided to measure maximum stress as a main criterion. The displacements was checked as an additional information for better understanding of the upper limb behaviour under load. Determination of the time of occurring of the highest maximum stress and displacement for the arm was applied for finding its localisation and for investigations of the state of the rest of the bones. Table 2 presents the maximum stress that occurs in the step 4 (Figure 6b) and displacement values occurring in the step 6 (see Figure 6b) the during the forward fall for three forearm positions.

Table 2. Maximal von Mises stress and displacement for different forearm positions.

		Humerus	Radius	Ulna	Load step	Time [s]
Pronation	von Mises stress [Mpa]]	15.77	84.7	57.51	4	0.072
	Displacement [mm]	0.019	5.48	5.57	6	0.423
Neutral	von Mises stress [Mpa]]	7.27	102.36	67.09	4	0.08
	Displacement [mm]	0.001	5.49	5.58	6	0.45
Supination	von Mises stress [Mpa]]	9.59	84.65	63.31	4	0.08
	Displacement [mm]	0.75	0.77	4.02	6	0.338

Figure 6. Maximum von Mises stress at forearm positions a) pronation, b) neutral, c) supination.

Maximum global displacement presents in Figure 8 occur in distal forearm.

Figure 7. Maximum displacement at forearm positions a) pronation, b) neutral, c) supination.

For all of compared positions, the highest stress was observed for the radius bone, while the lowest for humerus, what is compatible with the results from literature [6]. The placement of the fracture is dependent on position of the arm during the impact. For neural and supination positions the highest stress is in proximal radius.

The highest probability of the fracture is in the neutral position, as it shows the highest stress values during the fall. Investigations also resulted in obtaining displacement model and values of the bones in arm during the fall. In all cases displacement occurs in the distal forearm, however the bone that is moved depends on the fall position. In the cases of pronation and neutral positions the displacement values are nearly the same with nearly immobile humerus bone and the biggest displacement of the ulna. For supination position humerus and radius show small and nearly identical displacement, while the highest value is for ulna. The maximum von Mises stress and displacement values occurring for the nodes and the time histories of these quantities during fall are presented in Figures 7 and 8, respectively.

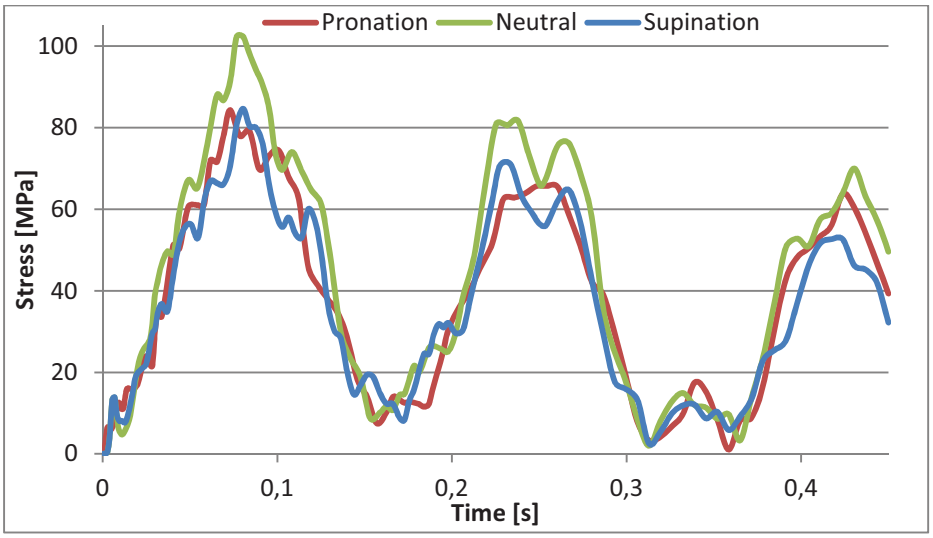

Figure 8. The resulted maximal von Mises stress in different forearm positions.

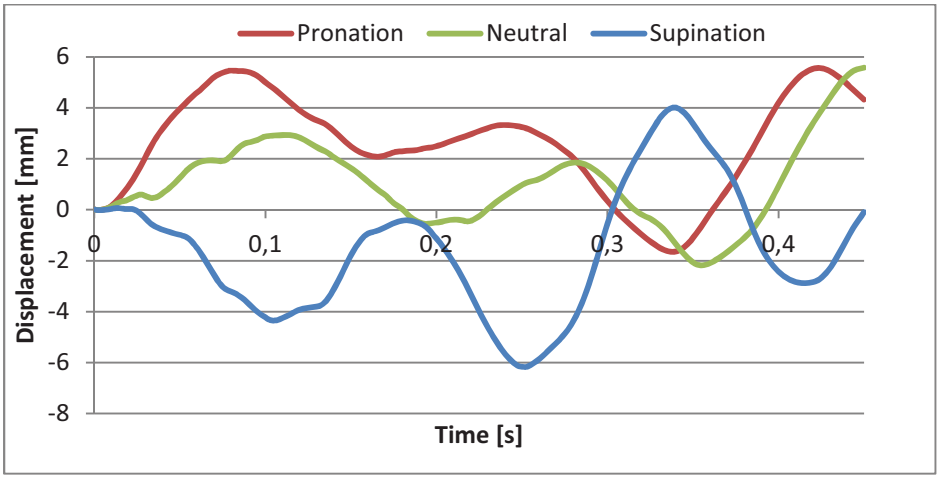

Figure 9. The resulted maximal displacement in different forearm positions.

4. Conclusions

This paper is a result of the introductory analysis of such a complex biomechanical system as a human upper limb. The aim of the research was to obtain results allowing for a better understanding of the dynamics of the bone injury during forward fall with straight arms.

Current state of the mathematical methods allowed to construct more precise models taking into account also influence of the muscles or ligaments. It is also possible to model joints using contact modeling, however lack of some of the parameters describing mechanical modelling of tissues is

problem in this kind of analysis. Also application of the FEM method can result in much more detailed models than those obtained via experimental techniques. Problems occurring during construction of realistic biomechanical models are compensated by the fact, that even less actual models are giving us possibility to analyse of the processes occurring in organisms, that are inaccessible to in vivo experiments.

Coupling degrees of freedom is simply method of connection bones in joints. Using this approach, we do know nothing about stress in joints, however it is not necessary for our analysis, as maximal stress occurs in distal forearm, at the fracture site [6,11,14]. The areas of greatest stress concentration and maximum strain were identified and results of numerical simulations are consistent with the literature [6,11,14]. Maximum von Mises stress does not occur in the maximal peak force in the first step, but in the fourth one (Figure 6b). It is related to the difference between the duration of the impulse applied by the impact and the bones free vibrations period. Simulation of the 1,5 m of the standing height fall was investigated by [14] and results shown that by increasing velocity of the fall by 75% causes the first peak force of GRF to be doubled reaching 2610 N. The second force peak force was also increased by 75% up to 800 N. It means that with the optimal velocity, even the fall from 1,5 m could cause fracture of the distal radius, as the magnitude of force necessary for fracture to occur is specified by authors at 2350 N [14]. In paper [15] presented is a method that can be applied to develop a set of models for distal radius fracture, which specifies a force necessary for bone breaking as 2142 N. The studies of the forward fall from 1 m with maximal peak force 1170 N, that are presented in this paper, were sufficient to determine locations of potential fractures and the obtained results that are consistent with literatures data [6,11,14]. Obtained results confirm that in the pronation position, that is the most popular during forward fall, the highest probability of the fracture in the distal radius.

References

1. Nevitt M.C., Cummings S.R.: Type of fall and risk of hip and wrist fractures: the study of osteoporotic fractures. The Study of Osteoporotic Fractures Research Group. *J. Am. Geriatr. Soc., 41, 1993, 1226-34.*
2. O'Neill T.W., Varlow J., Silman A.J., Reeve J., Reid D.M., Todd C., Woolf A.D.: Age and sex influences on fall characteristics. *Ann. Rheum. Dis., 53, 1994, 773-5.*
3. Vellas B.J., Wayne S.J., Garry P.J., Baumgartner R.N.: A two-year longitudinal study of falls in 482 community-dwelling elderly adults. *J. Gerontol A. Biol. Sci. Med. Sci., 53, 1998, 264-274.*
4. Hsio E.T., Robinovitch S.N.: Common protective movements govern unexpected falls from standing height. *Journal of Biomechanics, 31, 1998, 1-9.*
5. Mrozowski J., Awrejcewicz J.: *Introduction to Biomechanics*. Lodz, TUL Press, 2004 (in Polish).
6. Oskam J., Kingma J., Klasen J.: Fracture of the distal forearm: epidemiological developments in the period 1971 - 1995. *Injury, 29, 1998, 353 - 355.*
7. Feerick M.F., Kennedy J., Mullett H., FitzPatrick D., McGarry P.: Invastigation of metallic and carbon fibre PEEK fracture fixation devices for three-part proximal humeral fractures *Medical Engineering & Physics, 35*, 2013, 712 – 722.

8. Sun W., Starly B., Nam J., Darling A.: Bio-CAD modeling and its applications in computer-aided tissue engineering. *Computer-Aided Design, 37, 2005, 1097-1114.*
9. Rho J.Y., Hobatho M.C., Ashman R.B.: Relations of mechanical properties to density and CT number in human bone *Medical Engineering & Physics,*17, 1995, 347-355.
10. DeFrate L.E., Li G., Zayontz S.J., Herndon H.H, McGarry P.: A minimally invasive method for the determination of force in the inter osseous ligament *Clinical Biomechanics, 16*, 2001, 895 – 900.
11. DeGoede K.M., Ashton-Miller J.A.: Biomechanical simulations of forward fall arrests: effects of upper extremity arrest strategy, gender and aging – related declines in muscle strength. *Journal of Biomechanics, 36*, 2003, 413 - 420.
12. Tejszerska D., Mańka I.: *Modeling the lateral curvature of the human spine*. Gliwice, Silesian University of Technology Press, 2010 (in Polish).
13. User's Guide ANSYS 12, Ansys, Inc., Houston, USA.
14. Kim K.J., Ashton-Miller J.A.: Segmental dynamics of forward fall arrests: A system identification approach. *Clinical Biomechanics,* 24, 2009, 348 - 354.
15. Burkhart T.A., Andrews D.M., Dunning C.E: Multivariate injury risk criteria and injury probability scores for fractures to the distal radius. *Journal of Biomechanics,* 46, 2013, 973 - 978.

Paweł Biesiacki, M.Sc. (Ph.D. student): Lodz University of Technology, Department of Automation, Biomechanics and Mechatronics, Stefanowskiego 1/15, 90-537, Lodz, Poland, the author gave a presentation of this paper during one of the conference sessions (800045@edu.p.lodz.pl).

Jan Awrejcewicz, Professor: Lodz University of Technology, Department of Automation, Biomechanics and Mechatronics, Stefanowskiego 1/15, 90-537, Lodz, Poland (jan.awrejcewicz@p.lodz.pl).

Jerzy Mrozowski, Ph.D: Lodz University of Technology, Department of Automation, Biomechanics and Mechatronics, Stefanowskiego 1/15, 90-537, Lodz, Poland (jmrozow@p.lodz.pl).

Krzysztof Woźniak, Ph.D.: Jagiellonian University Medical College, Department of Forensic Medicine, 31-531 Kraków, Grzegórzecka 16, POLAND (mpwoznia@cyf-kr.edu.pl).